Supplementary Information

Supporting Information for the paper entitled "Electronic Delocalization in Small Water Rings" by Bo Wang, Minsi Xin, Xing Dai, Ruixia Song, Yan Meng, Jie Han, Wanrun Jiang, Zhigang Wang* and Ruiqin Zhang*.

1. The isolated single water ring (ISWR) initial structures
2. Water cluster vibrational characteristics in infra-red (IR) and Raman spectra
3. Energy level diagrams from MP2 and M062X calculations
4. Results of the population analysis of the molecular orbitals
5. Molecular orbitals contribution of the isolated water molecule
6. Nuclear independent chemical shift (NICS) zz curves of water rings for n=3-6
7. Second order perturbation theory analysis of Fock matrix with NBO basis
8. Analysis of hydrogen (H)-bond lengths and angles
9. Analysis of the Natural Bond Orbitals (NBO) and Mulliken charges of oxygen (O) atoms in water clusters
10. References for supplementary information

1. The ISWR initial structures

To prepare the calculations and analyses of the ISWR, we first built initial structures containing virtual atoms (see Figure S2) in order to allow the O atom at the same plane to relax. The exo-ring H of the structures containing an even number of water molecules lie in the up-down position (an unusual orientation for H) with respect to the stable main structure, while the corresponding H atoms in structures comprising an odd number of water molecules exist at the up-up position in a stable structure.

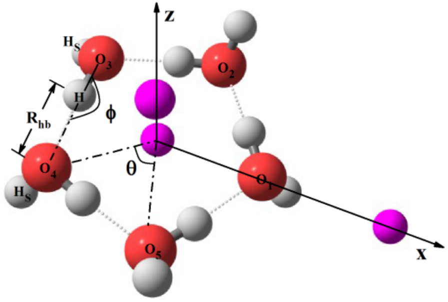

Figure S1 Schematic diagram of a typical ISWR structure (O in red, H in white, H-bonds along the grey dotted lines and three virtual atoms in pink).

To unify the numbering, we label the H-bond in the water molecule containing O_3 pointing to the O_4 as the first H-bond and the numbers of the other H-bonds in the ring increase in the counterclockwise direction. In this work, all statistics are performed according to this definition. R_{hb} represents the H-bond distance between the donor H and acceptor O atoms, φ the bond angle (∠OHO), θ the central angle formed by the two O atoms and one virtual atom, H_S the H atoms with the same orientation, H the H atom forming the H-bond, and O_1-O_5 the water molecules, numbered beginning with the one at the X axis. The reference axes are established based on the positional relationships of the three virtual atoms (rendered in pink).

2. Water cluster vibrational characteristics in the IR and Raman spectra

IR and Raman spectroscopies are widely used to describe the structural properties of water clusters. We calculated the vibration spectra of stable water ring structures with n=3-6 and obtained their Raman and IR spectra. These were consistent with previous reports.[8,S1,S2] The corresponding peak frequencies of the Raman spectra are 3569.8 cm^{-1}, 3498.7 cm^{-1}, 3255.00 cm^{-1}, and 3234.9 cm^{-1} for n=3-6, respectively, as shown in Figure S2a. These peaks have the same vibration mode; that is, the overall H-bond stretching mode. We found that the highest peak presented a red shift with the increase in the number of water molecules (n) when n≤6, indicating a trend for the bond strength to decline.

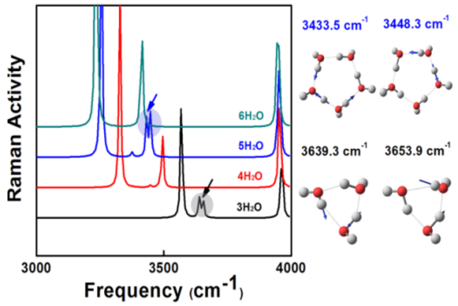

Figure S2a The solid lines, from bottom to top, denote the Raman spectra for the water rings of $(H_2O)_3$, $(H_2O)_4$, $(H_2O)_5$, and $(H_2O)_6$. The shadow areas indicated by the blue and black arrows represent the characteristic peaks of two kinds of ring structures. The right panel illustrates the four spectral vibrational modes of the water ring for $(H_2O)_3$ and $(H_2O)_5$, and the corresponding modes can be found in the left panel.

In Figure S2a, the shaded areas of the peaks to which the black and blue arrows point correspond to the characteristic water ring vibration modes for n=3 and 5 (see Figure S2a for the vibration mode diagram in the right panel). The peaks of the black curve of 3639.3 cm-1 and the blue curve of 3433.5 cm^{-1}, respectively, correspond to the OH bonds stretching away from the water molecules with the same orientations. The peaks of the black curve at 3653.9 cm-1 and the blue curve at 3448.3 cm^{-1}, respectively, are the OH bond stretching modes from the water molecules with the same orientation. Compared with the Raman spectroscopy, the IR spectroscopy also shows some qualitative trends.

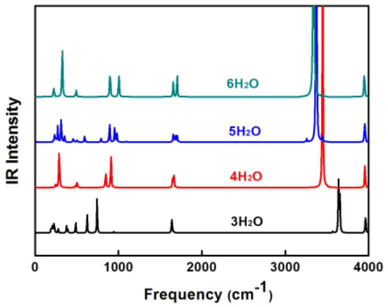

Figure S2b The solid curves, from bottom to top, denote the IR spectra for the water rings of $(H_2O)_3$, $(H_2O)_4$, $(H_2O)_5$, and $(H_2O)_6$.

In Figure S2b, the peaks of the IR spectra can be classified into three regions; (1) the vibration modes below 1100 cm^{-1} corresponding to the relative movements between the water molecules and the OH bond of water in an intramolecular asymmetric twist; (2) the vibration mode in the range 1000-2000 cm^{-1} denotes the symmetrical swing of the H and O atoms; and (3) the main vibrational mode in the frequency above 3000 cm^{-1} represents the stretching modes between the intermolecular and intramolecular form of the OH bond. The highest peaks of the water ring structures are found at the frequencies 3639.3 cm^{-1}, 3447.3 cm^{-1}, 3366.0 cm^{-1}, and 3337.9 cm^{-1}, respectively. They have the same vibrational modes corresponding to the vibration of the OH bonds. We can see that the highest peaks show red shifts as the number of water molecules increases toward 6.

3. Energy level diagrams from MP2 and M062X calculations

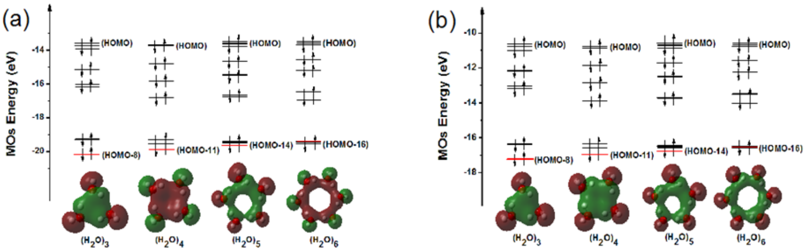

Figure S3 The energy level diagrams of water clusters from MP2(a) and M062X(b) calcuations.

Figures S3a and S3b represent the MP2 and M062X calculation results including the energy levels of water rings and selected characteristic occupied MOs. The energy levels of the latter are marked with red lines in the diagram. The isosurface value of the orbital diagram is 0.02 a.u. As shown in Figure S3, the features of the energy level diagram and the trend of the orbitals in the two sets of results are consistent and also consistent with those obtained from PBE0 calculations.

4. Results of the Population Analysis of the Molecular Orbitals

Table S1 The atomic orbital contribution percentages in HOMO-(8,11,14,16) correspond to the special molecular orbitals indicated in Figure 1 of the $(H_2O)_3$, $(H_2O)_4$, $(H_2O)_5$, and $(H_2O)_6$. p represents the valence orbital contribution of an O atom, s_H the s-orbital contribution of an H atom forming the H-bond, and s the s-orbital contribution of the free H atom.

$(H_2O)_3$ (HOMO-8)			$(H_2O)_4$ (HOMO-11)			$(H_2O)_5$ (HOMO-14)			$(H_2O)_6$ (HOMO-16)		
O (%)	H (%)		O (%)	H (%)		O (%)	H (%)		O (%)	H (%)	
2p	$1s_H$	1s	2p	$1s_H$	1s	2p	$1s_H$	1s	2p	$1s_H$	1s
76.01	10.17	13.37	76.29	9.56	13.72	76.37	9.30	13.88	76.64	10.01	12.89

Their contribution percentages are listed in Table S1. The linear combination of the molecular orbitals of different fragments (that is, different water molecules) gives the molecular orbital structure shown in Figure S4, where the p-orbital component also varies due to the structural differences. From the orbital analysis, the total contribution made by the 2p and 1s orbital electrons is basically the same as that of the isolated water molecule in Figure S4.

5. Molecular orbitals contribution of the isolated water molecule

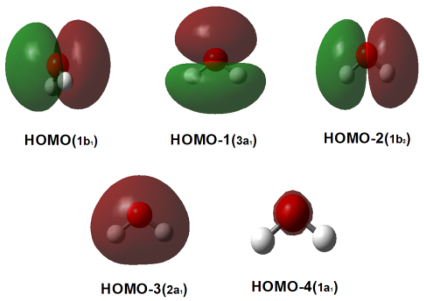

Figure S4 The molecular orbitals of the isolated water molecule.

The nth orbital below the highest occupied molecular orbital (HOMO) is denoted by HOMO-n. The corresponding irreducible representation of the molecular orbitals is also shown in Figure S4. The results of the calculation are consistent with recent experimental data.[S3] It can clearly be seen that the molecular orbital in Figure 1 is HOMO-2 which is a linear combination of H and O atomic orbitals. The 2p orbital contribution of the O atom accounts for about 74.32% of the OH bond, and the 1s orbital contributions of the two H atoms are about 12.62% and 12.62%, respectively.

6. Nuclear independent chemical shift (NICS) zz curves of water rings for n=3-6

NICS and NICSzz values are widely used to probe the aromaticity in electron delocalized systems, with the latter being more reliable.[S4,S5,S6] Here we constructed NICSzz curves of water rings for n=3-6 and benzene (C_6H_6), which are shown in Figures S5a and S5b, respectively. The NICSzz curve of benzene is given as a common reference, and it is consistent with previous studies.[S7,S8] Different from benzene, water rings show antiaromaticities around centers of rings and aromaticities at other regions. Both antiaromaticity and aromaticity decrease with the increase of number (n) of water molecules. The trend also involves some difference between the cases of n=3 and 4 and n=5 and 6 (see Fig. S5a). Each of the cases of n=3 and 4 presents a valley at about 2 Å from the center of the water ring, showing the region with maximum aromaticity. But, the valley is hardly observed in the curves of n= 5 and 6. This further illustrates the difference between small water rings and large water rings.

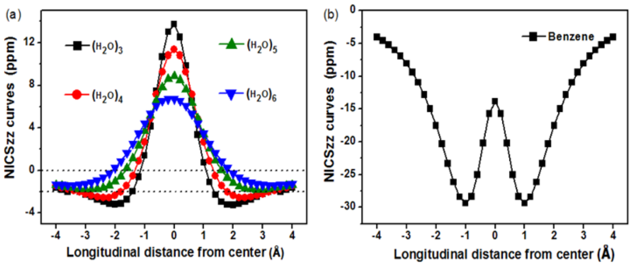

Figure S5. Nuclear independent chemical shifts (NICS) as function of the longitudinal distance from the center of the water rings for n=3-6 (Figure S1a) and benzene (C_6H_6; Figure S1b), respectively.

7. Second order perturbation theory analysis of Fock matrix with NBO basis

We performed a complete NBO analysis. The large values of stabilization energy E(2) are presented in Table S2. NBO analysis shows that the stabilization energy E(2) increases gradually with the increase of the number of water molecules. This interaction weakens the O-H bond and elongates the O-H (namely, contracted O…H). This result is in agreement with the previous studies,[S9,S10] and the trend is consistent with the previous one that the H-bond length decreases gradually with the increase of the number of water molecules.[6,20]

Table S2. Second order perturbation theory analysis of Fock matrix with NBO basis.

	Donor (i)	**Nature orbital occupancy**	**Acceptor (j)**	**E(2)[a] (kJ/mol)**	**E(j) − E(i)[b] (a.u.)**	**F(i,j)[c] (a.u.)**
$(H_2O)_3$	**$LP_2(O_1)$** 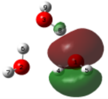	1. 96832	**$BD^*(O_3- H_8)$** 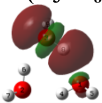	**14.75**	**1.01**	**0.109**
	$LP_2(O_2)$ 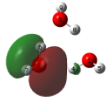	1. 97127	**$BD^*(O_1–H_4)$** 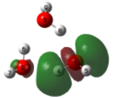	**13.06**	**1.01**	**0.103**
	$LP_2(O_3)$ 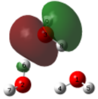	1. 96725	**$BD^*(O_2– H_6)$** 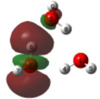	**14.93**	**0.99**	**0.109**
$(H_2O)_4$	**$LP_2(O_1)$**	**1.94891**	**$BD^*(O_4–H_{11})$**	**25.53**	**1.01**	**0.144**

	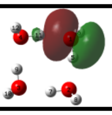		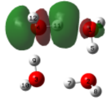			
	$LP_2(O_2)$ 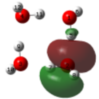	**1.94882**	**$BD^*(O_1–H_5)$** 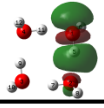	**25.63**	**1.02**	**0.144**
	$LP_2(O_3)$ 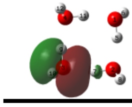	**1.94877**	**$BD^*(O_2–H_7)$** 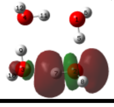	**25.67**	**1.02**	**0.144**
	$LP_2(O_4)$ 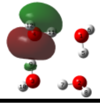	**1.94886**	**$BD^*(O_3–H_9)$** 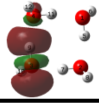	**25.61**	**1.02**	**0.144**
$(H_2O)_5$	**$LP_2(O_1)$** 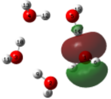	**1.94289**	**$BD^*(O_5–H_{14})$** 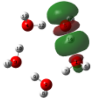	**29.48**	**1.04**	**0.156**
	$LP_2(O_2)$ 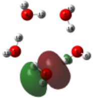	**1.94255**	**$BD^*(O_1–H_7)$** 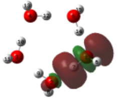	**29.54**	**1.03**	**0.156**
	$LP_2(O_3)$ 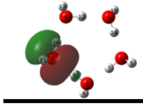	**1.94395**	**$BD^*(O_2–H_9)$** 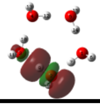	**29.11**	**1.05**	**0.156**
	$LP_2(O_4)$ 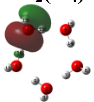	**1.94691**	**$BD^*(O_3–H_{10})$** 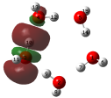	**27.34**	**1.06**	**0.152**
	$LP_2(O_5)$ 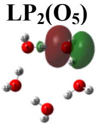	**1.94273**	**$BD^*(O_4–H_{12})$** 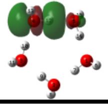	**29.41**	**1.03**	**0.156**
$(H_2O)_6$	**$LP_2(O_1)$** 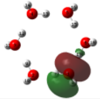	1.93329	**$BD^*(O_6–H_{17})$** 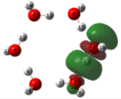	**34.31**	1.01	0.166
	$LP_2(O_2)$ 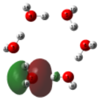	1.93367	**$BD^*(O_1–H_7)$** 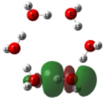	34.12	1.01	0.166
	$LP_2(O_3)$ 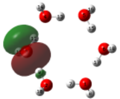	1.93339	**$BD^*(O_2–H_9)$** 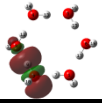	34.20	1.01	0.166
	$LP_2(O_4)$ 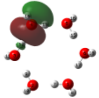	1.93355	**$BD^*(O_3–H_{12})$** 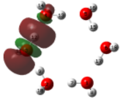	34.16	1.01	0.166
	$LP_2(O_5)$ 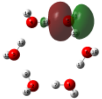	1.99727	**$BD^*(O_4–H_{13})$** 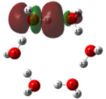	34.24	1.01	0.166

$LP_2(O_6)$ 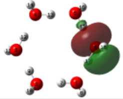	1. 93340	$BD^*(O_5–H_{15})$ 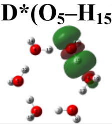	34. 23	1. 01	0. 166

[a] E(2) stands for the stabilization energy. [b] energy difference between donor and acceptor (i_{th} and j_{th} NBO orbitals). [c] F(i,j) is the Fock matrix element between i_{th} and j_{th} NBO orbitals.

8. Analysis of H-bond lengths and angles

Table S3 H-bond length R_{oh} (Å)

$(H_2O)_3$	**1.879**	**1.853**	**1.853**			
$(H_2O)_4$	**1.721**	**1.721**	**1.721**	**1.723**		
$(H_2O)_5$	**1.702**	**1.685**	**1.684**	**1.684**	**1.686**	
$(H_2O)_6$	**1.678**	**1.678**	**1.678**	**1.677**	**1.677**	**1.677**

Table S4 Bond angle (∠O-H…O) Φ(°)

$(H_2O)_3$	**147.2**	**149.9**	**149.8**			
$(H_2O)_4$	**166.8**	**166.9**	**166.8**	**167.1**		
$(H_2O)_5$	**174.2**	**177.0**	**176.2**	**176.4**	**176.5**	
$(H_2O)_6$	**176.8**	**176.8**	**176.8**	**176.8**	**176.8**	**176.8**

In Table S3, the data in the columns and diagonals (enclosed with dashed lines) increase as the number of water molecules decreases. The decrease in H-bond lengths for n=3-6 is consistent with previous results.[6,20] As we can see from the column and diagonal terms (enclosed with dashed lines) in Table S4, the bond angle Φ(∠OH…O) increases gradually with the increase of the number of water molecules.[6,20]

9. Analysis of the Mulliken and NBO charges of O atoms in water clusters

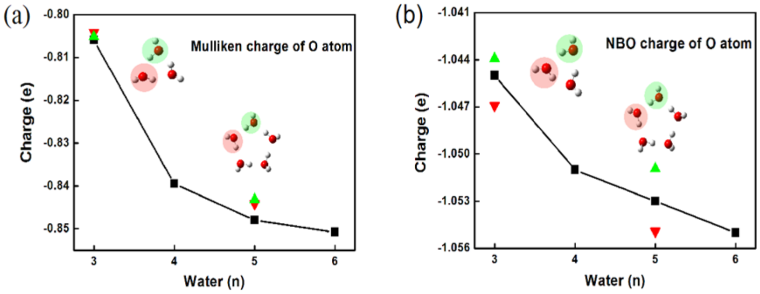

Figure S6 (a, b) represent the Mulliken and NBO charges of the O atom.

The black boxes represent the average Mulliken (or NBO) charges of the O atoms at n = (4,6) or the average Mulliken (or NBO) charges for the removal of the O atoms of the same orientation at n=3 and 5. The red and green areas represent the Mulliken (or NBO) charges of the O atom in the same orientation. Figure S6 (a, b) shows the Mulliken and NBO charges of the O atom, which demonstrate a similar trend for n=3-6. However, the Mulliken or NBO charges of the O atom show an obvious change at n=3 and 4.

10. References for Supplementary Information

S1. J. R. Reimers and R. O. Watts, *Chem. Phys.* 1984, **85**, 83.
S2.H.Cybulski,and J. Sadlej, On the calculations of the vibrational Raman spectra of small water clusters. *Chem. Phys.* 2007, **324**, 163.
S3. J. Guo, X. Meng, J. Chen, J. Peng, J. Sheng, X. Z. Li and Y. Jiang, *Nat. Mater.* 2014, **13**, 184.
S4. J. Yu, Q. Sun, Y. Kawazoe, P. Jena, *Nanoscale,* 2014, **6,** 14962.
S5. R. Gershoni - Poranne, A. Stanger, *Chem.-Eur. J.*, 2014, **20,** 5673.
S6. A. C. Tsipis, *Phys. Chem. Chem. Phys.,* 2009, **11,** 8244.
S7. A. Stanger, *J. Org. Chem.* 2006, **71,** 883.
S8. Z. Chen, C. S. Wannere, C. Corminboeuf, R. Puchta, P. V. R. Schleyer, *Chem. Rev.,* 2005, **105,** 3842.
S9. J. Chocholoušová, V. Špirko, P. Hobza, *Phys. Chem. Chem. Phys.*, 2004, **6,** 37.
S10. S. V. C. Vummaleti, D. Branduardi, M. Masetti, M. De Vivo, R. Motterlini, A. Cavalli, *Chem.-Eur. J.*, 2012, **18,** 9267.